Journal of Engineering and Applied Sciences 14 (2): 516-525, 2019
ISSN: 1816-949X

Effect of Time Fixing Aluminum (In its Solid State Phase): On Recovery Rate of a Memory Alloy (Cu, Al, Ni)

Ahmed Abdulrasool Ahmed Alkhafaji
Department of Mechanical Engineering, College of Engineering, University of Baghdad,
Baghdad, Iraq

Abstract: Shape memory alloys (Cu+Al+Ni) can be applied in many scientific fields, the alloy is manufactured by Powder Metallurgy (P/M) method. The sintering stage is performed in two stages. The 1st stage is to stabilize the solid phase of the aluminum, this is done by keeping the temperature at the 1st stage at 500°C for 1 h. This is performed, so, as to ensure that the aluminum does not change to a molten state when passing through the 2nd sintering stage at which the alloy is heat treated at 850°C. This research studied the effect of the heat treatment time on shape recovery. The alloy used was [83% Cu-13% Al-4% Ni]. Three different time periods were used for the 1st stage of the heat treatment and they were (0.5, 1.0, 1.5 h) the recovery was treatment time of (1.0 h) then 0.5 h and lastly 1.5 h. Physical tests were also performed to ensure that both martensite and austenite were present. The recovery rates were 80, 25 and 10% , respectively, for the three times to stay samples. This study shows the importance of the amount of time spent on the 1st stage of the sintering process for this type of alloy for the recovery percentage.

Key words: (Cu-Al-Ni) smart alloys, powder metallurgy, strain recovery, XRD, SEM, martensite, method

INTRODUCTION

Shape memory alloys are alloys that regain their original deformed shape after heat has been applied. The transformation of martensite from high temperature parent symmetric austenite phase to low temperature less symmetric martensite phase (Dasgupta *et al.*, 2014) is responsible for this behavior. When cooling the sample without applying load to the material transforms from austenite to twinned martensite. When heating the opposite transformation will occur as shown in Fig. 1. While Fig. 2 shows the transformation with mechanical loading (shape recovery effect) (Kumar and Lagoudas, 2008). Cu based alloy is good with high temperature application because of its high temperature application (46-146°C) (Benke *et al.*, 2009).

This behavior has made these alloys important in the field of research especially, since, they can be applied in important scientific fields such as space, medicine and safety equipment. Most of these alloys are manufactured in a manner Powder Metallurgy (P/M).

Zhu *et al.* (2007) studied copper-aluminum and nickel prepared from pure powder using Mechanical Alloying (MA) technique the microstructures of shape memory powders of copper aluminum nickel were studied using the means of hardness measurement, metallography observation, X-ray diffraction and Scanning Electron Microscope (SEM).

Balo and Sel (2012) investigated the effect of thermal aging at constant temperature above the austenite transformation final temperature upon heating on the martensite transformation of Cu-13.5, Al-4% Ni shape memory alloy.

Mustafa (2013) studied to improve Cu-Al-Ni SMAs properties by controlling the transformation temperatures to be used in applications of different working temperatures, especially, at high temperature applications.

By Alfay *et al.* (2014) fabricated shape memory alloy Copper Aluminum-Nickel samples using powder metallurgy under control atmosphere (with tube furnace and vacuum sintering environment). Nb was added to master alloys Cu-Al-Ni in three ranges (0.3, 0.6, 0.9%) weight percentage.

By Esra *et al.* (2015), mechanical and physical properties of Cu based shape memory alloy with a chemical composition of 83, Cu-13, Al-4% Ni was investigated, after adding three alloying elements (Sn, Ti and V) in three weight percent (0.4, 0.8 and 1.2% wt.) for each element were added to obtain nine alloys.

By Abdulrasool and Sarah (2016), the mixing materials weight percentage is 83, Cu-13, Al-4% wt. Ni. Has been followed by the compacting process. The powder compacted with three different values of the pressure (300, 500, 700) MPa. The sintering process was in a tube and vacuum furnace. They were at three different values of sintering temperatures (700, 800, 900°C) necessary and

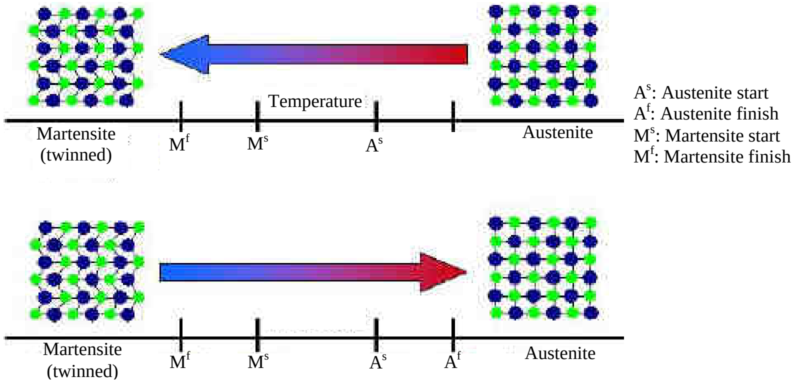

Fig. 1: Temperature induced phase transformation of a shape memory alloy without mechanical loading (Kumar and Lagoudas, 2008)

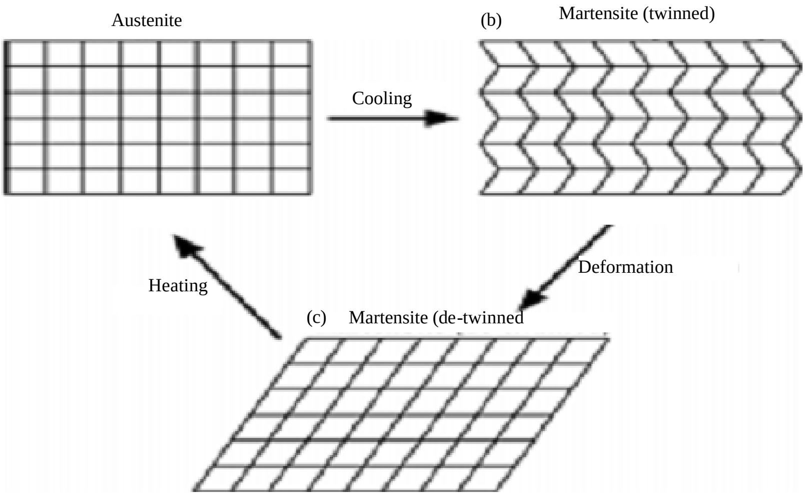

Fig. 2: Martensitic and austenitic change upon heating and cooling (Kumar and Lagoudas, 2008)

testing for screening of resilience and examination of compression for all samples were v carried out. The highest resilience value at 700 Mpa and at a sintering temperature of 900°C either check compression straight was the highest value at a pressure of 300 MPa and temperature found that sintering 900°C.

Abdulrasool and Abdulsahib (2017) found that there is no physical relationship between porosity and shape recovery. They used Powder Metallurgy (P/M) to manufacture Cu-13, Al-4% Ni alloy. By producing 5 samples every sample sintered in difference sintering time (3-7 h). The samples also heat treated to stabilize Martensite phase. The result of shape recovery and porosity testing analyses by using artificial neural network predicting system to predict shape recovery and porosity behavior between 3 and 7 h sintering hours with smaller time step. By Abdulrasool and Bassam (2018) two elements (Cu, AL) of the alloy (Cu-Al-Ni) on the physical and mechanical properties which is considered one of the smart materials. This alloy has a standard weight percentage in [83 Cu-13, Al-4% Ni]. Selecting four different weight percentages of elements (Cu-Al) include [78, Cu,18% Al], [80, Cu, 16% Al] [82, Cu, 14% Al] and [84, Cu,12% Al]. The results of the sample test show the maximum values of shape recovery and micro hardness are 83%, 185 HV, respectively which appeared in the weight percentage [82, Cu-14, Al-4% Ni] whereas the samples in the weight percentages [78, Cu-18, Al-4% Ni], [80, Cu-16, Al-4% Ni] don't appear any shape recovery because of increasing brittleness and decreasing toughness with increase Al% content which lead into failure in these proportions.

By Ammar and Al-Khafaji (2018). This research, the newly achieved results determined the best ratio of (Cu-Ni) and (Al-Ni) in the smart (Cu-Al-Ni) alloys since these values achieved the best results in terms of, hardness and porositythe experimental results obtained in this reasurch showed that when there is an increase in Al and Ni concentration in alloy lead, it will automatically increase the hardness and porosity but the increase in Al ratio showed that it is more effect than that of the increase of the Ni ratio.

This research focuses on the change of time in the initial stage of thermal treatment at a temperature of 500°C. It is through our reading of previous research that we did not get the research stopped at this point.

MATERIALS AND METHODS

Powder preparation: Cu-Al-Ni was prepared by powder metallurgy method. The powder which has been used in this study was brought from (Skyspring Nanomaterials, USA) with a purity of 99% and an average particle size of 45 μ (-325 mesh). The first step was to mix the powder of Cu83-Al13-Ni4% by horizontal drum mixing with 78 rpm speed for 6 h with with 1% acetone (by volume) to prevent particle separateration due to different densities also acetone decreases the friction between particles Fig. 3 shows the horizontal drum that was used for mixing the powder.

Compacting: Powder mixture was compacted at 650 MPa using cylindrical die of 11 mm diameter. These sample dimensions are (11 mm dia. ×5 mm length) and (11 mm dia. ×16.5 mm length) shown in Fig. 4 and 5. The compacting process from two sides to increase the homogeneity of density along the sample. After compacting finish the punch put on hold at 650 MPa for 2 min to prevent the spring back of the sample as shown in Fig. 6. In this research, produced 9 samples, 6 samples have (11 dia. ×16.5 mm length) and 3 samples have (11 dia. ×5 mm length). Figure 7 shows the two type of samples that were manufactured. The optical microscopy with 200×was then used to investigate the microstructure of the samples after compacting as shown in Fig. 8-10.

Sintering: The compacted samples were then sintered in two stages. Samples divided in three sets to be sintered in the first stage at 500°C, heating rate of 15°C/min from room temperature, all sets have 3 samples 2 with a length 16 mm and one has a 5 mm length (for hardnes test). Different time of these sets is holding it this stage (0.5, 1, and 1.5 h), respectively. Because the Al melting point is 660°C. The second stage for all sets have the same condition of sintering at 850°C hold it 5 h, for every sample directly after the first stage, heating rate (10°C/min) to reach this after the first stage, Fig. 3 shows the diagram of sintering procedure. Then samples were left to cool in furnace to room temperature for the purpose

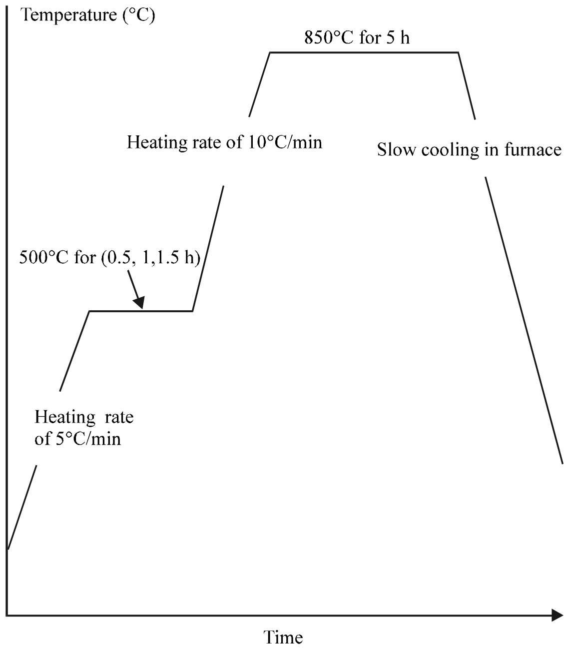

Fig. 3: Diagram of sintering procedure

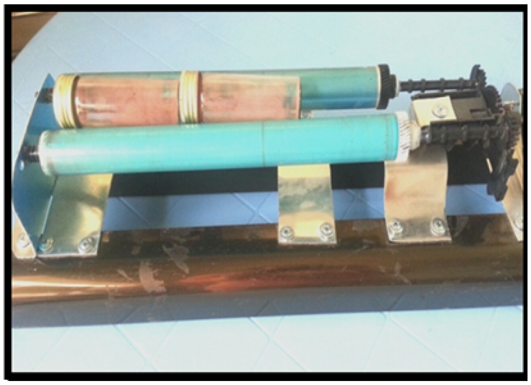

Fig. 4: Horizontal drum mixing

Fig. 5: Die, punch and holder for mold

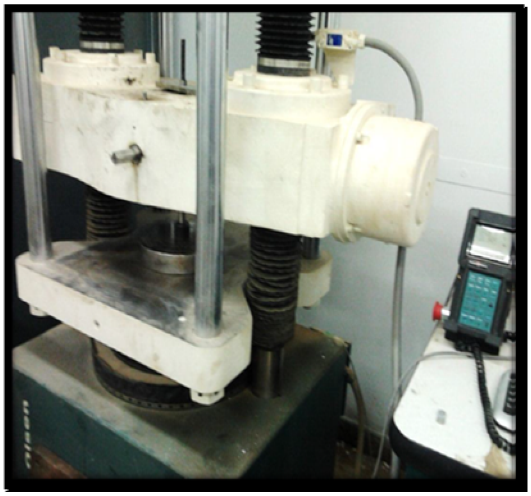

Fig. 6: Uniaxial press machine

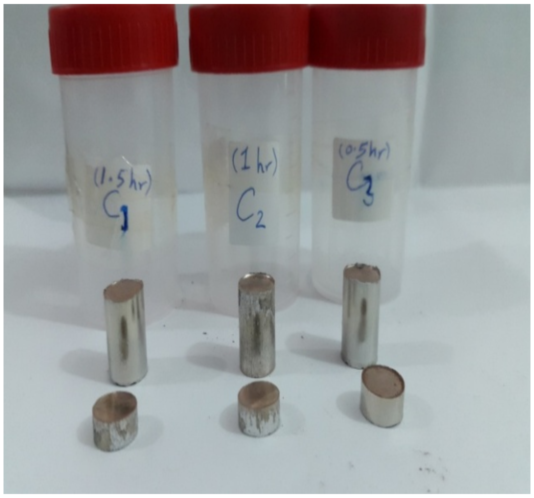

Fig. 7: Tow type of sample manufacturing

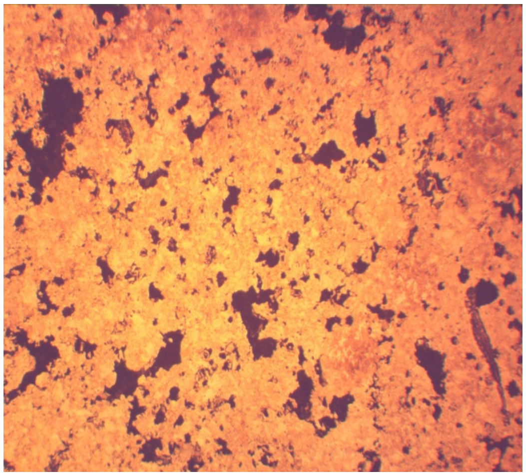

Fig. 8: Microstructure of sample C_1 after compacting

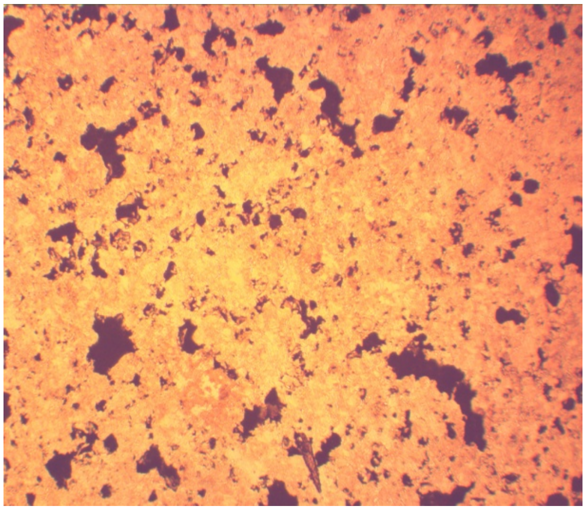

Fig. 9: Microstructure of sample C_2 after compacting

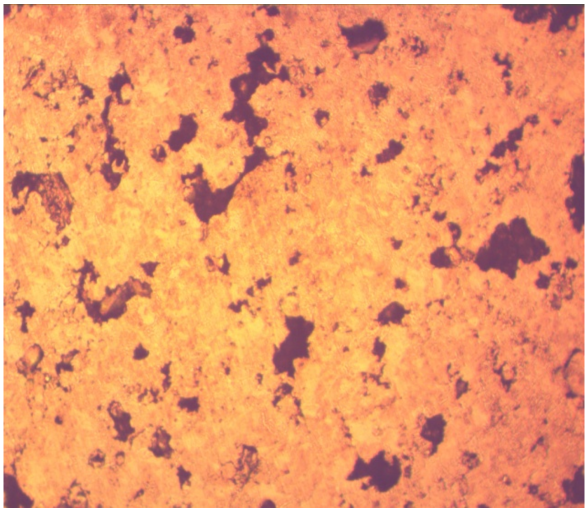

Fig. 10: Microstructure of sample C_3 after compacting

of bonding particles of the sample in the solid state. The sintering process was done an electrical tube furnace with a vacuum atmosphere to prevent oxidization of the samples, Fig. 11 shows the furnace and Fig. 12 shows the samples after sintering.

Heat treatment procedure: By the same system (electrical tube furnace with a vacuum atmosphere to prevent oxidization of the samples) was used for all samples in three groups. To transform the austenite samples after sintering to Martensite, two stages of heat treatment were employed. The first stage (aging the samples at 800°C hold it at 1 h and after that rapidly quenched in iced water). And the second stage (heating the samples to 100°C and hold it for 2 h and left it to cool in furnace).

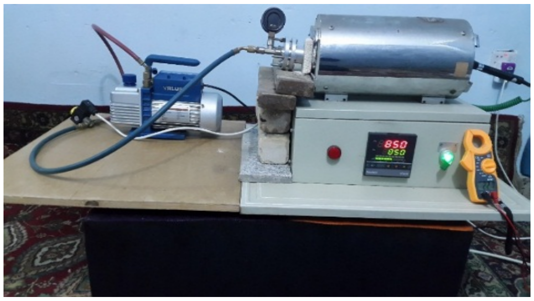

Fig. 11: Electrical furnace with a vacuum system

Fig. 12: Samples after sintered

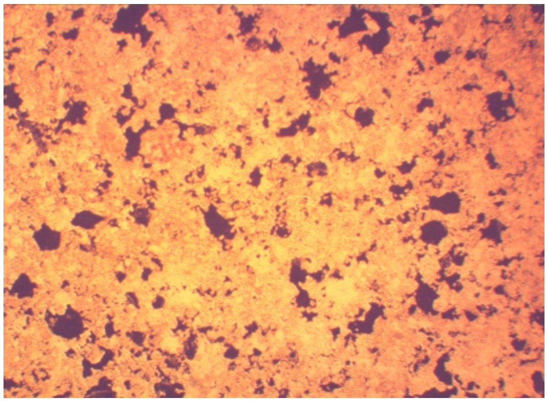

Fig. 13: Microstructure of sample (C_1) after sintering

Tests after manufacturing: After etching the samples, so, as to prepare them for microscopic inspection the following tests were performed.

Physical tests: Optical microscopy this test was done to show the homogeneity of the samples after compacting and sintering, Fig. 8-10 show the microstructure of samples (C_1-C_3) after compacting and Fig. 13-15 show the microstructure of samples (C_1-C_3) after sintering.

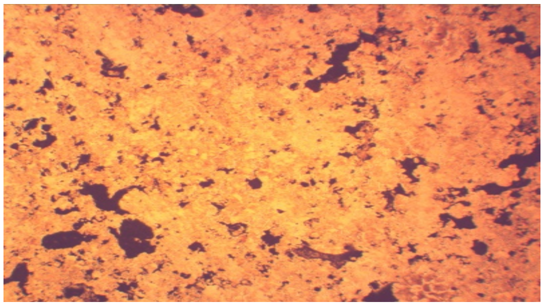

Fig. 14: Microstructure of sample (C_2) after sintering

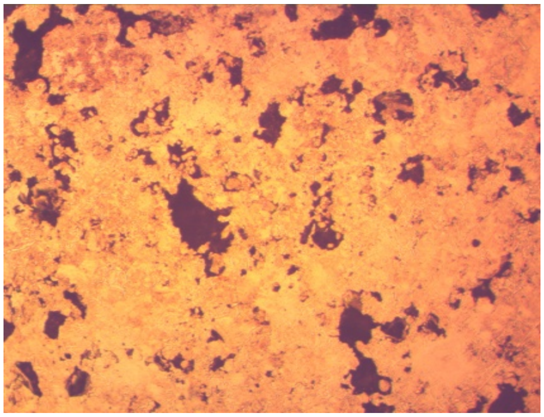

Fig. 15: Microstructure of sample (C_3) after sintering

XRD: X-ray diffraction tests were done on samples (C_1-C_3) before and after sintering, to cover the range of changes in first stage sintering time. The purpose of mentioned test was for investigating the effect of sintering time on martensite transformation because the martensite transformation is the most important step to ensure that the sample is a smart alloy. Figure 16-18 show the results of these tests. SEM: scanning electron microscope was used to obtain clear observation on microstructure to see the Martensite phase as shown in Fig. 19-21.

Mechanical tests: Shape Memory Effect (SME or strain recovery) test was used the same press machine and vacuum furnace system. Equation 1 was used to calculate the Shape Memory Effect ratio (SME%) (Wan *et al*., 2002):

$$\text{SME\%} = [\,(L_2\text{-}L_1)/(L_0\text{-}L_1)]\times 100 \qquad (1)$$

Where:

L_0 = Original Length (mm)

L_1 = Length after compacted (mm)

L_2 = Length after heating (mm)

(a)

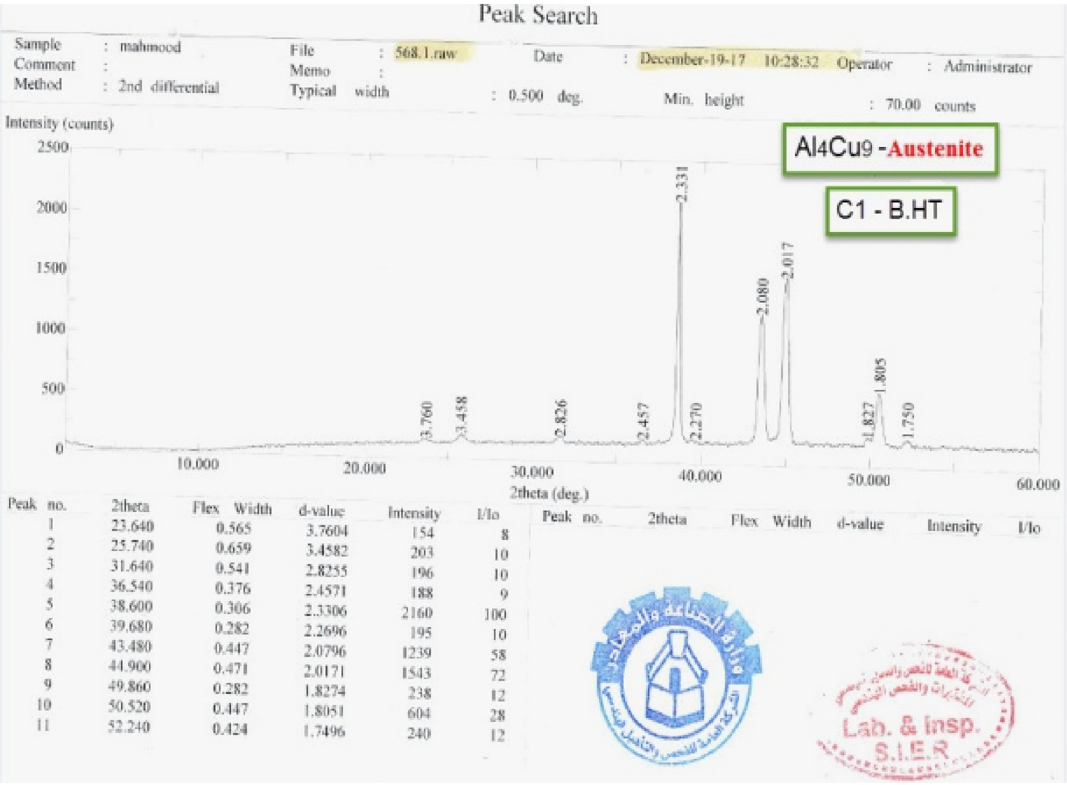

Peak Search

Sample : mahmood
Comment :
Method : 2nd differential
File : 568.1.raw
Memo :
Typical width : 0.500 deg.
Date : December-19-17 10:28:32
Operator : Administrator
Min. height : 70.00 counts

Peak no.	2theta	Flex Width	d-value	Intensity	I/Io
1	23.640	0.565	3.7604	154	8
2	25.740	0.659	3.4582	203	10
3	31.640	0.541	2.8255	196	10
4	36.540	0.376	2.4571	188	9
5	38.600	0.306	2.3306	2160	100
6	39.680	0.282	2.2696	195	10
7	43.480	0.447	2.0796	1239	58
8	44.900	0.471	2.0171	1543	72
9	49.860	0.282	1.8274	238	12
10	50.520	0.447	1.8051	604	28
11	52.240	0.424	1.7496	240	12

(b)

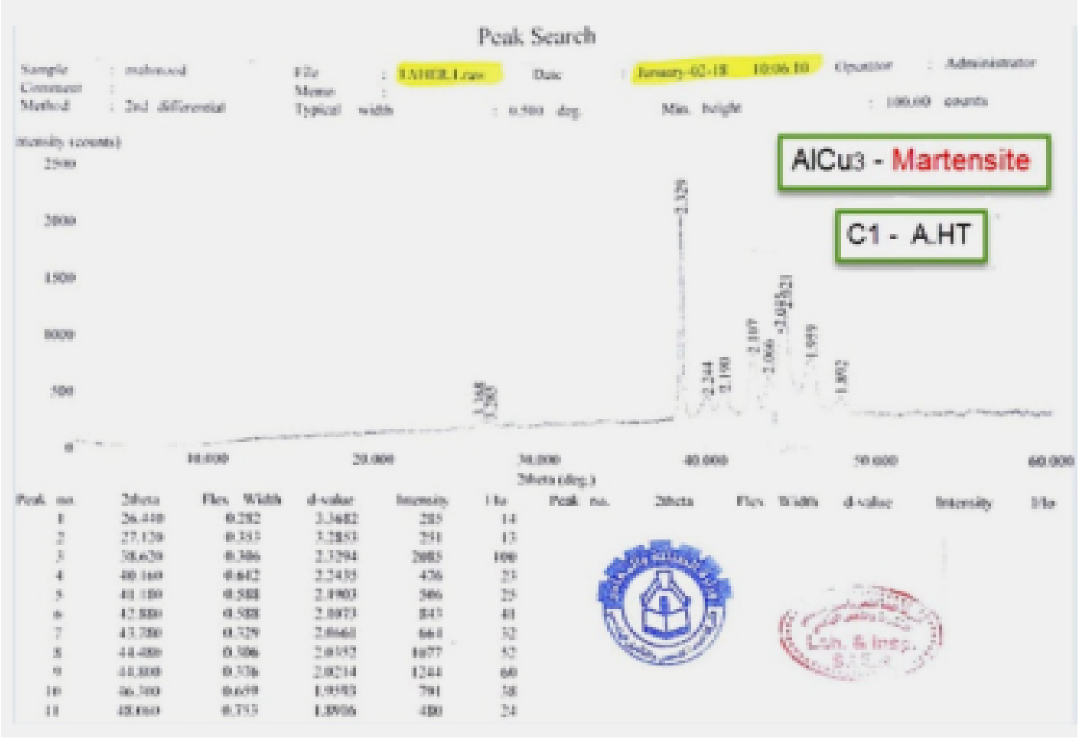

Peak Search

Sample : mahmood
Comment :
Method : 2nd differential
File : TAHER.1.raw
Memo :
Typical width : 0.500 deg.
Date : January-02-18 10:06:10
Operator : Administrator
Min. height : 100.00 counts

Peak no.	2theta	Flex Width	d-value	Intensity	I/Io
1	26.440	0.282	3.3682	285	14
2	27.120	0.353	3.2853	251	13
3	38.620	0.306	2.3294	2083	100
4	40.160	0.642	2.2435	476	23
5	41.180	0.588	2.1903	506	25
6	42.880	0.588	2.1073	843	41
7	43.780	0.329	2.0661	661	32
8	44.480	0.306	2.0352	1077	52
9	44.800	0.376	2.0214	1244	60
10	46.300	0.659	1.9593	791	38
11	48.060	0.753	1.8906	480	24

Fig. 16: XRD tests before and after sintering for sample C_1: a) C_1 before sintering and b) After sintering

(a)

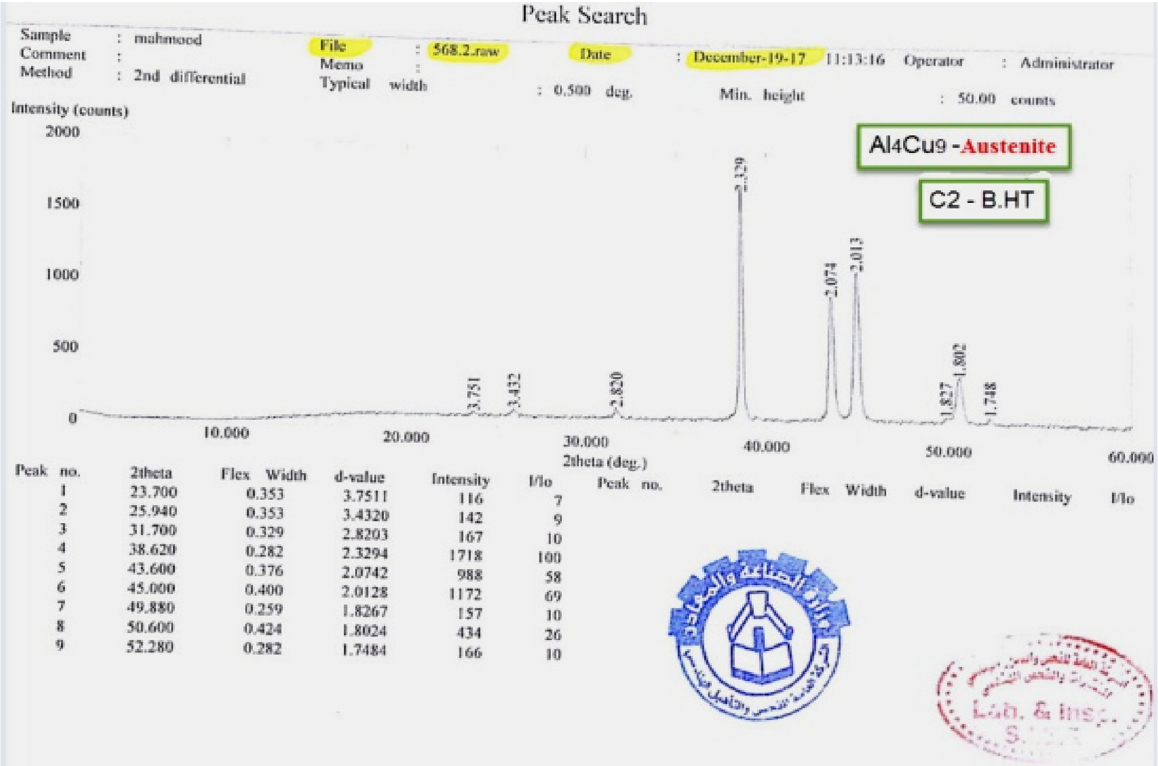

Peak Search

Sample : mahmood
Comment :
Method : 2nd differential
File : 568.2.raw
Memo :
Typical width : 0.500 deg.
Date : December-19-17 11:13:16
Operator : Administrator
Min. height : 50.00 counts

Peak no.	2theta	Flex Width	d-value	Intensity	I/Io
1	23.700	0.353	3.7511	116	7
2	25.940	0.353	3.4320	142	9
3	31.700	0.329	2.8203	167	10
4	38.620	0.282	2.3294	1718	100
5	43.600	0.376	2.0742	988	58
6	45.000	0.400	2.0128	1172	69
7	49.880	0.259	1.8267	157	10
8	50.600	0.424	1.8024	434	26
9	52.280	0.282	1.7484	166	10

(b)

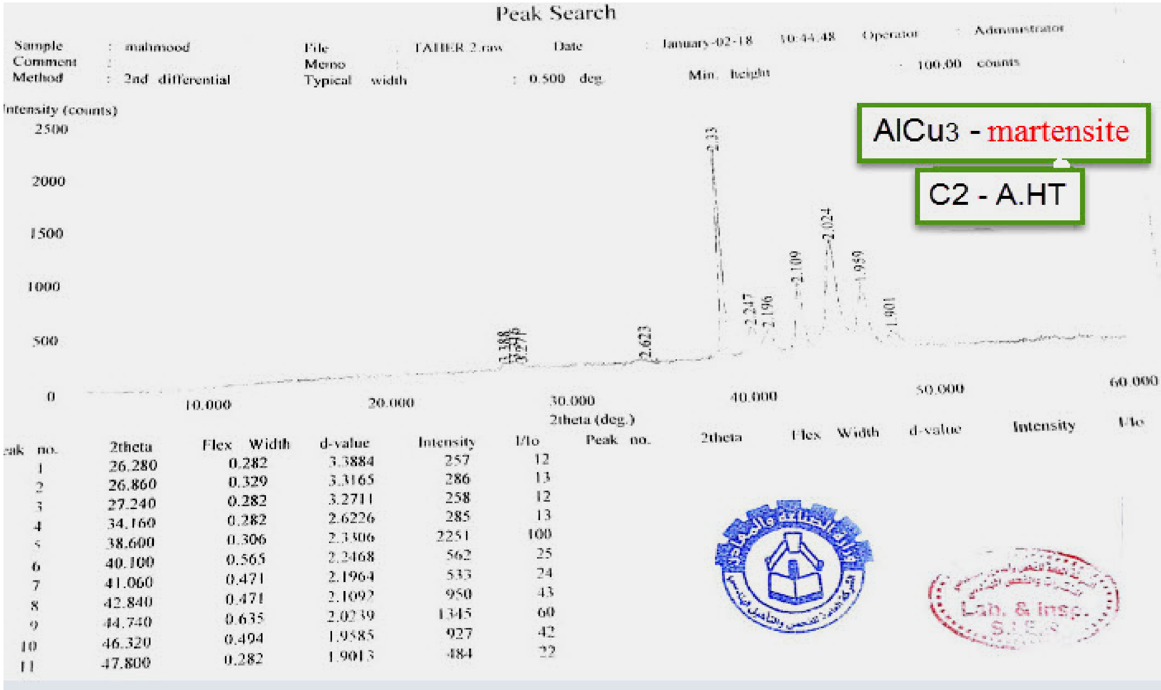

Peak Search

Sample : mahmood
Comment :
Method : 2nd differential
File : TAHER 2.raw
Memo :
Typical width : 0.500 deg.
Date : January-02-18 10:44:48
Operator : Administrator
Min. height : 100.00 counts

Peak no.	2theta	Flex Width	d-value	Intensity	I/Io
1	26.280	0.282	3.3884	257	12
2	26.860	0.329	3.3165	286	13
3	27.240	0.282	3.2711	258	12
4	34.160	0.282	2.6226	285	13
5	38.600	0.306	2.3306	2251	100
6	40.100	0.565	2.2468	562	25
7	41.060	0.471	2.1964	533	24
8	42.840	0.471	2.1092	950	43
9	44.740	0.635	2.0239	1345	60
10	46.320	0.494	1.9585	927	42
11	47.800	0.282	1.9013	484	22

Fig. 17: XRD tests before and after sintering for sample C_2: a) C_2 before sintering and b) C_2 after sintering

(a)

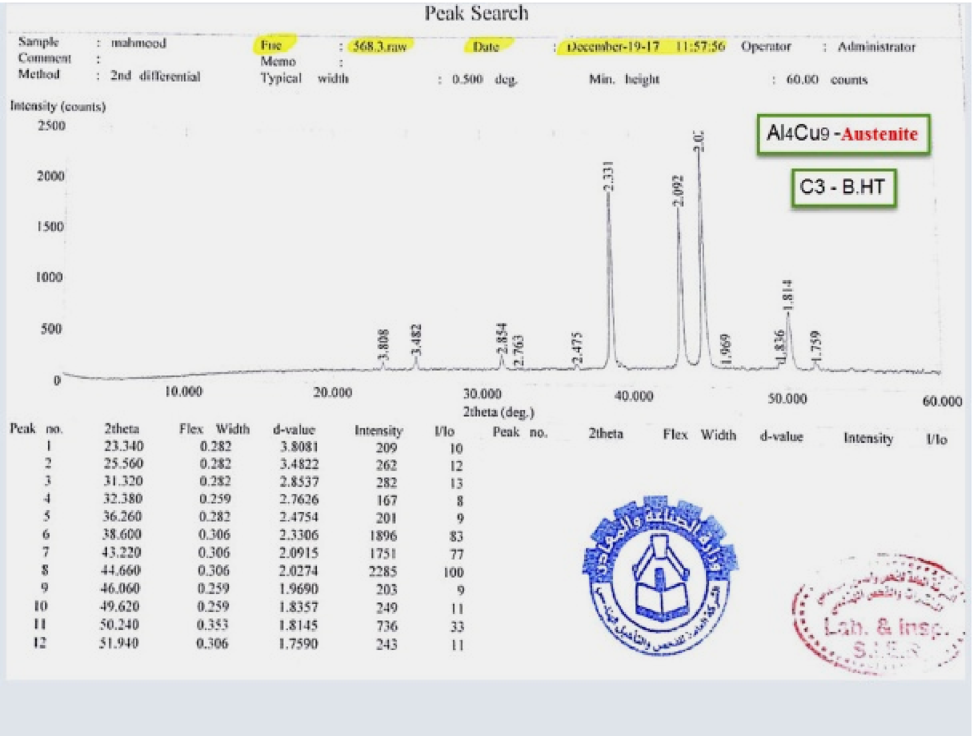

Peak Search

Sample : mahmood
Comment :
Method : 2nd differential
File : 568.3.raw
Memo :
Typical width : 0.500 deg.
Date : December-19-17 11:57:56
Min. height : 60.00 counts
Operator : Administrator

Peak no.	2theta	Flex Width	d-value	Intensity	I/Io	Peak no.	2theta	Flex Width	d-value	Intensity	I/Io
1	23.340	0.282	3.8081	209	10						
2	25.560	0.282	3.4822	262	12						
3	31.320	0.282	2.8537	282	13						
4	32.380	0.259	2.7626	167	8						
5	36.260	0.282	2.4754	201	9						
6	38.600	0.306	2.3306	1896	83						
7	43.220	0.306	2.0915	1751	77						
8	44.660	0.306	2.0274	2285	100						
9	46.060	0.259	1.9690	203	9						
10	49.620	0.259	1.8357	249	11						
11	50.240	0.353	1.8145	736	33						
12	51.940	0.306	1.7590	243	11						

(b)

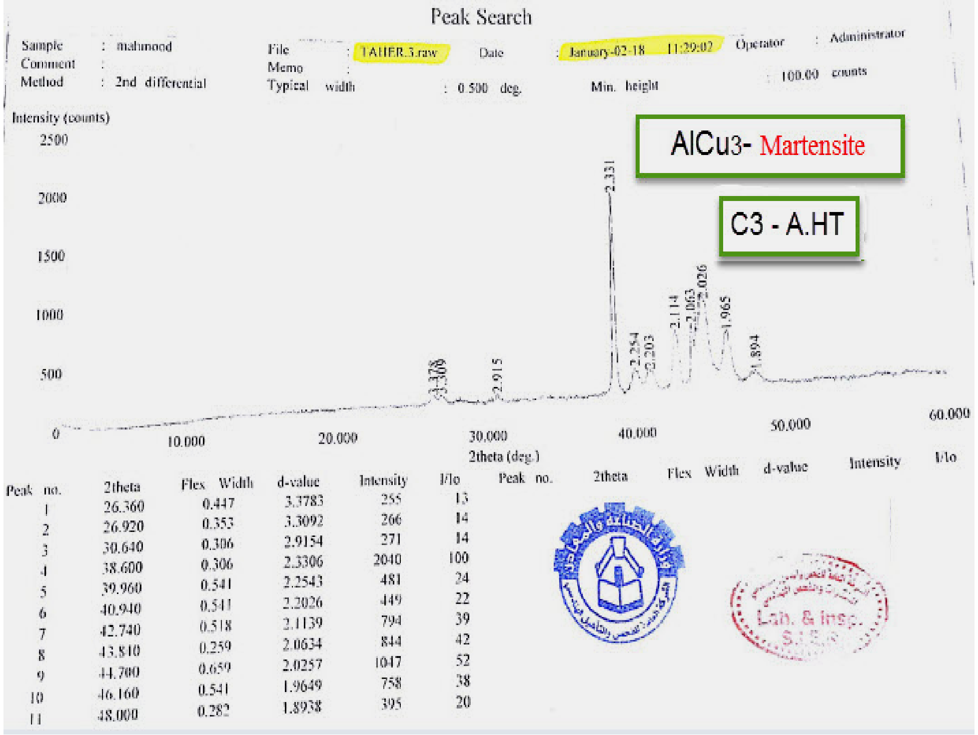

Peak Search

Sample : mahmood
Comment :
Method : 2nd differential
File : TAHER.3.raw
Memo :
Typical width : 0.500 deg.
Date : January-02-18 11:29:02
Min. height : 100.00 counts
Operator : Administrator

Peak no.	2theta	Flex Width	d-value	Intensity	I/Io	Peak no.	2theta	Flex Width	d-value	Intensity	I/Io
1	26.360	0.447	3.3783	255	13						
2	26.920	0.353	3.3092	266	14						
3	30.640	0.306	2.9154	271	14						
4	38.600	0.306	2.3306	2040	100						
5	39.960	0.541	2.2543	481	24						
6	40.940	0.541	2.2026	449	22						
7	42.740	0.518	2.1139	794	39						
8	43.810	0.259	2.0634	844	42						
9	44.700	0.659	2.0257	1047	52						
10	46.160	0.541	1.9649	758	38						
11	48.000	0.282	1.8938	395	20						

Fig. 18: XRD tests before and after sintering for sample C_2: a) C_3 before sintering and b) C_3 after sintering

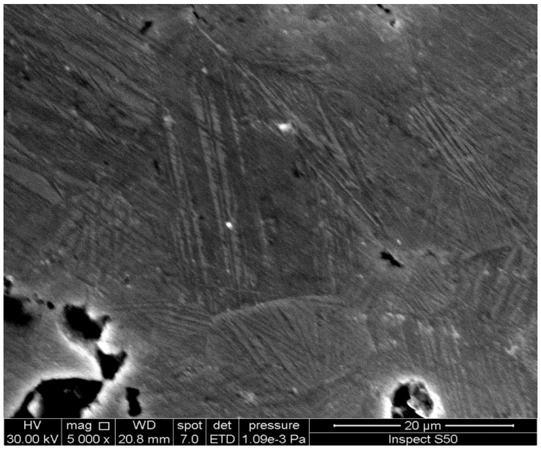

Fig. 19: SEM after sintering sample C_1

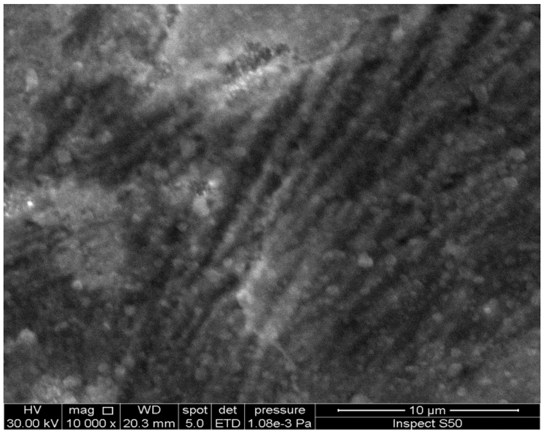

Fig. 20: SEM after sintering sample C_2

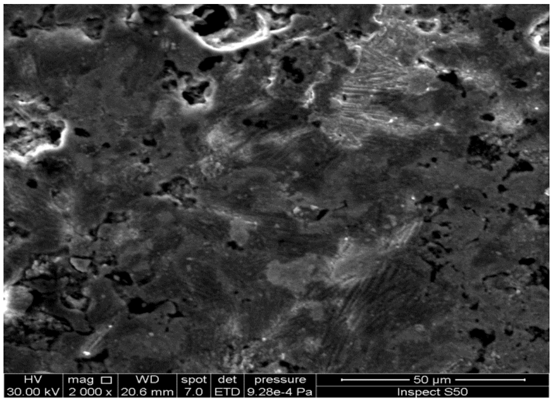

Fig. 21: SEM after sintering sample C_3

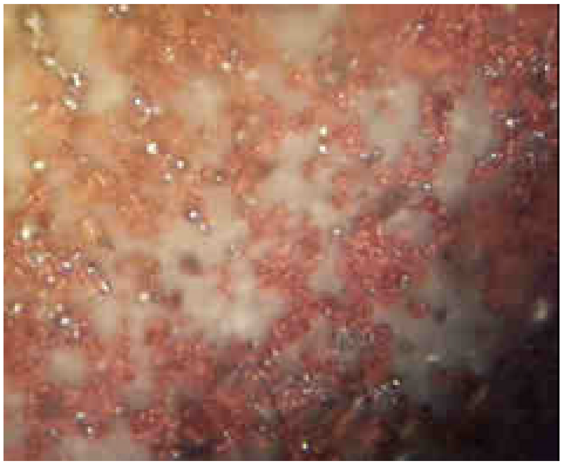

Fig. 22: Particles after mixing

Table 1: Sme% results of samples under study

Sample No.	Sintering time (h) of first stage	L_o (mm)	L_1 (mm)	L_2 (mm)	SME (%)
C_1	1.5	15.940	15.790	15.805	10.00
C_2	1.0	15.630	15.120	15.530	80.39
C_3	0.5	14.240	14.200	14.210	25.00

Micrometer was used in measuring lengths after calibration in this test compacted the samples (C_1-C_3) (martensitic phase) by 4% from the original length (L_o), measure length after compacted (L_1), we put the samples in the vacuum furnace system, heated to a temperature of 250°C for 5 min, then taken out to the air to cool to obtain austenite phase, measure the length after heating (L_2), apply Eq. 1 to find the shape memory effect ratio Table 1 shown SME% results (Fig. 22).

RESULTS AND DISCUSSION

In the mixing stage of the metal powders used in the manufacture of the samples have the ability to remember its manufacturing shape (SMA), the weight ratios of the specific components must be precisely because it has an effect on the physical and mechanical properties as well as the speed and time of the mixing stage. The process of homogenization of the ingredients of the mixture gives the same specifications as possible to the samples. To make sure, the optical microscope is checked to ensure the homogeneity of the components before the compaction, Fig. 22 show the particles after mixing.

After compacting, the optic microscopy testing image shows the compacting efficiency, the distribution and homogeneity of alloying elements for all samples as shown in Fig. 8-10. Black spaces in images indicate porosity, high porosity is evidence that the pressure is insufficient to ensure bonding force between particles.

X-ray diffraction tests were done on samples (C_1- C_3) before sintering (Fig. 16-18). The presence of the austenite (Al_4Cu_9) phase in all samples. After sintering with different times of the first stage, the XRD tests presence of the martensite ($AlCu_3$) phase in all samples, Fig. 16-18 after sintering this is the influential phase of the alloy. Figure 13-15 show the microscopic structure of the samples after sintering, there was no significant difference in color for the three samples. But there is a diminishing pore size and a better spread. There is no effect of the difference in the time of fouling of the first stage on the microscopic structures after the completion of the sintering.

SEM tests (Fig. 19-21) show the martensite layer that was tested by the SEM device at a first stage sintering time of (1.5, 1 and 0.5 h). The Martensite is clearer in samples sintered at (1.5 and 1 h). This is due to the more time spent on sintering the more diffusion will take place.

The objective of the research is to know the effect of the sintering time of the first stage on the SME. Table 1 explains the results of the SME examination. The lowest recovery rate was at 1.5 h with a value of 10% then it improved by a significant amount at the time of 1 h at 80% SME when the time is reduced by half the hour decreased but by a better increase of 1.5 h, the value SME 25% at 0.5 h. From this we conclude that the stabilization time of the aluminum phase has a significant effect on the amount.

CONCLUSION

The main conclusion of this research is to investigate the effect of time staying on the samples in the first stage. The optimum keeping time at the designated temperature was 60 min, it gave the best recovery shape percentage. When a higher or lower time staying other than the optimumal found (60 min), even though keeping it more then 60 min gave better shape recovery the keeping it more than 60 min it was still not as good as 60 min.

The percentage differences of the components of this three component composition or adding other elements to it. May lead to different time for sintering of the first stage, this means that attention should be paid to the study of this stage when the ratios change.

Ensure the presence of phases (austenite and martensite) responsible for restoring the shape before and after sintering. It is important before completing the processes of heat treatment and mechanical tests.

REFERENCES

Abdulrasool, A. and H. Abdulsahib, 2017. Investigation on relationship between shape memory effect and interconnection porosity under multiple sintering time of smart alloy Cu-Al-Ni. Assoc. Arab Univ. J. Eng. Sci., 24: 77-87.

Abdulrasool, A. and J.M. Sarah, 2016. Effect of compaction pressure and sintering temperature on shape effect and compression strength of Cu-Al-Ni shape memory alloy. Assoc. Arab Univ. J. Eng. Sci., 23: 1-17.

Abdulrasool, A. and S.D. Bassam, 2018. Effect of Cu-Al proportions in smart (Cu-Al-Ni) alloy for best mechanical properties by using artificial intelligent. Assoc. Arab Univ. J. Eng. Sci., 25: 11-22.

Alfay, R.Z., M.T. Ayad and K.A.A.A. Rahim, 2014. Effect of Nb addition on hardness and wear resist of Cu-Al-Ni shape memory alloy fabricated by powder metallurgy. J. Eng., 20: 42-49.

Ammar, T.M. and A.A. Al-Khafaji, 2018. Effect of (Al-Ni) and (Cu-Ni) concentrations ratios on the hardness and porosity of ternary (Cu-Al-Ni) smart alloys. Aust. J. Basic Appl. Sci., 12: 36-48.

Balo, S.N. and N. Sel, 2012. Effects of thermal aging on transformation temperatures and some physical parameters of Cu-13.5 wt. % Al-4 wt. %Ni shape memory alloy. Thermochim. Acta, 536: 1-5.

Benke, M., V. Mertinger and L. Daroczi, 2009. High-Temperature transformation processes in Cu-13.4Al-5Ni shape memory alloy single crystals. J. Mater. Eng. Perform., 18: 496-499.

Dasgupta, R., A.K. Jain, P. Kumar, S. Hussein and A. Pandey, 2014. Effect of alloying constituents on the martensitic phase formation in some Cu-based SMAs. J. Mater. Res. Technol., 3: 264-273.

Esra, A.A., S.A. Shakir and M.T. Ayad, 2015. Experimental study on the physical and mechanical properties of Cu-Al-Ni shape memory alloys. MSc Thesis, Al-Mustansiriya University, Baghdad, Iraq.

Kumar, P.K. and D.C. Lagoudas, 2008. Introduction to Shape Memory Alloys. In: Shape Memory Alloys, Kumar, P.K. and D.C. Lagoudas (Eds.). Springer, Boston, Massachusetts, USA., ISBN:978-0-387-47684-1, pp: 1-51.

Mustafa, A.M., 2013. Studying shape memory effects of Cu-Al-Ni alloys. MSC Thesis, Department of Production Engineering and Metallurgy, University of Technology, Baghdad, Iraq.

Wan, J., X. Huang, S. Chen and H.X.Z. Ty, 2002. Effect of nitrogen addition on shape memory characteristics of Fe-Mn-Si-Cr alloy. Mater. Trans., 43: 920-925.

Zhu, X., L. Zhou, F. Mei, L.U.O. Ming and G.O.N.G. Shen *et al*., 2007. Structure evolution of Cu-based shape memory powder during mechanical alloying. Trans. Nonferrous Met. Soc. China, 17: 1422-1427.